

Dynamic Coupling Analysis of E-type Membrane for Six-Axis Force Sensor

^{1,2} Xie LIFENG, ^{1,2} Xu DEZHANG

¹ School of Mechanical and Automotive Engineering, Anhui Polytechnic University, Wuhu, 241000, China

² Advanced Numerical & Servo Technology, Anhui Polytechnic University, Wuhu, 241000, China

E-mail: 304246668@qq.com

Received: 10 September 2013 / Accepted: 25 October 2013 / Published: 30 November 2013

Abstract: The E-type membrane which is used for measuring forces in other five directions will generate coupling outputs and influence accuracy of the sensor, when six-axis force sensor based on double layer E-type membrane is under dynamic loads in M_z direction. In terms of the fundamental theory of mechanical vibration, vibration mechanics and elastic mechanics, this paper simplifies the E-type membrane into a straight circular shaft with constant section and works out the coupling outputs under the condition of dynamic loads. It provides theoretical basis for dynamic decoupling of six-axis force sensor. *Copyright* © 2013 IFSA.

Keywords: Six-axis force sensor, E-type membrane, Shaft, Coupling, Dynamic decoupling.

1. Introduction

With the development of robot technology in the direction of high speed, high accuracy and intelligent, research on the dynamics of robot has been paid more and more attention [1]. Sensor technology is the kernel which influences the development of robot in these areas. Therein, six-axis force sensor (6-AFS) which can measure all forces and torque in three-dimensional space is one of the most important robot sensors [2]. 6-AFS based on double layer E-type membrane which the Institute of Intelligent Machines, Chinese Academy of Sciences (CAS) owns the proprietary intellectual property rights, takes a monolithic structure [3]. It exists coupling effect among dimensions in the process of measurement. Therefore, dynamic coupling problem of 6-AFS must be solved.

Over the years, the solution of dynamic coupling problem can be divided into two types. One is

achieving a more accurate result by means of mathematics algorithm which is used for compensating the coupling outputs [4]. The other one is building the mechanical models on the basis of the elastomer structures, extracting the characteristics of dynamic coupling and finishing the dynamic decoupling [5]. It is obviously that the latter one is more accurate. Circular thin plate is one of the most important elastomers of 6-AFS based on double layer E-type membrane. There is a lot of dynamic analysis of it. P. A. A. Laura et al. consider the case of transverse vibration of an annular plate with an intermediate circular support and a free inner edge. Z. H. Zhou et al. deal with the natural vibration of thin circular and annular plates using Hamiltonian approach. S. Stoykov et al. investigate the geometrically nonlinear free vibrations of thin isotropic circular plates using a multi-degree-of-freedom model, which is based on thin plate theory and on Von Karman's nonlinear strain-displacement

relations. Vinayak Ranjan et al. involve the determination of the fundamental frequency of vibration of solid and annular circular plate with different boundary conditions and with point mass attached at an arbitrary position [6, 9]. From these references, we can see that researchers often analyze the so called transverse vibration which was perpendicular to the middle surface of the plate and calculate the fundamental frequencies while they investigate circular thin plates. There is little data for the solution of the torsional vibration problem that a couple of centrosymmetric dynamic loads acting on the circular thin plate, when the so called lengthways dynamic loads in M_z direction acting on the sensor.

This paper will simplify the circular thin plate of elastomers of 6-AFS into straight circular shaft with constant section on the basis of the fundamental theory of mechanical vibration, vibration mechanics and elastic mechanics. A novel solution of the torsional vibration problem of lamella is proposed. The dynamic coupling outputs of circular thin plate under dynamic loads in M_z direction is worked out and figures of dynamic three-dimensional strain is simulated with the help of the software MATLAB. The results have very important significance to dynamic performances recognition, dynamic decoupling and the improvement of the measurement of the sensor [10].

2. Structure of Six-Axis Force Sensor and Establishment of Mechanical Model

2.1. Structure of Six-Axis Force Sensor

This paper takes 6-AFS based on ultrathin double layer E-type membrane on as the object of the research, as shown in Fig. 1.

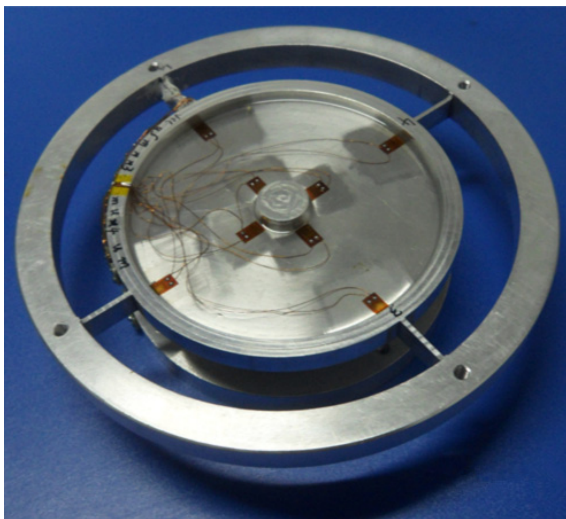


Fig. 1. Solid of the 6-AFS.

In order to facilitate analysis and calculation, this paper focuses on the simplified structure as shown in Fig. 2. Rectangular lamella 1, upper E-type membrane 4 and lower E-type membrane 6 are elastic structures. They will deform under the condition of dynamic loads. Upper force-transmitting loop 2, middle force-transmitting loop 3, central solid cylinder 5 and base frame 7 can be regarded as rigid bodies. They don't generate the deformation under the condition of dynamic loads. They are used for transferring the external loads.

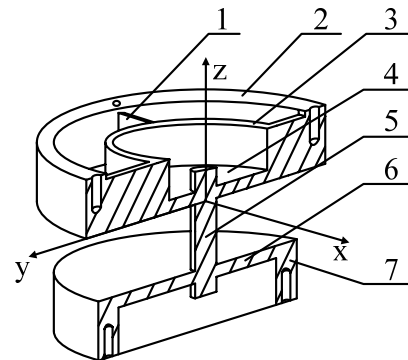


Fig. 2. Structure of the 6-AFS.

The structure as shown in Fig. 3 is the resistance strain gauge which is stuck on the elastomers of 6-AFS. It consists of insulation covering layer 1, metal resistance wires 2, basis material 3 and outgoing line 4. Its fundamental is that the elastomers will generate mechanical deformation under the condition of external loads, the strain gauges which are stuck on the elastomers will cause the resistance value change and the resistance value change will convert into electric current or voltage by the bridge.

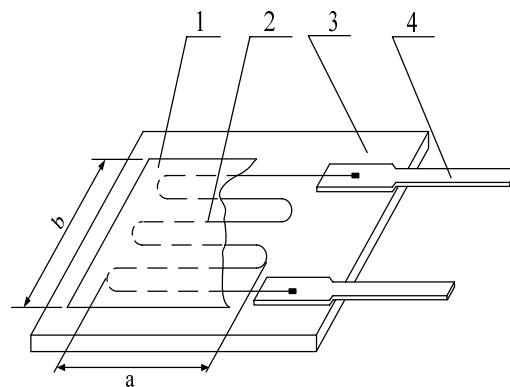


Fig. 3. Structure of the resistance strain gauge.

The relationship between resistance variation ΔR and strain ε is given by Equation (1):

$$S = \frac{\Delta R}{R} / \varepsilon \quad (1)$$

where the original resistance which is measured in the room temperature R and the sensitiveness coefficient of the strain gauge S can be seen as constant. Resistance variation is linearly related to strain in Equation (1). Therefore, strain of elastomers

under the dynamic loads can be regarded as outputs, while the dynamic coupling problem of the sensor is analyzed. For the parameters of E-type membrane, please refer to Table 1.

Table 1. Parameters of the sensor.

Material	r_i /[m]	r_o /[m]	l /[m]	ρ /[kg·m ⁻³]	G /[Pa]	J_ρ /[m ⁴]	a /[m]	b /[m]
LY12	7.5×10^{-3}	5×10^{-2}	2×10^{-3}	2.78×10^3	2.7×10^{10}	9.8125×10^{-6}	7.3×10^{-3}	4.4×10^{-3}

2.2. Establishment of Mechanical Model of the Elastomers

This paper analyzes the coupling strain output problem of 6-AFS under the dynamic loads in M_z direction. In the structure of 6-AFS, as shown in Fig. 1, rectangular lamella 1 is the elastomer which is used for measuring the dynamic loads in the main direction M_z . Upper and lower E-type membranes 4 and 6 are the elastomers which generate coupling outputs in the other five directions, when the dynamic load in M_z direction acts on the sensor.

According to the foregoing mechanical analysis, this paper simplifies upper E-type membrane into the model as shown in Fig. 4. The model is a straight circular shaft with constant section whose bottom is fixed and top is free under distributive torque $f(z,t)$.

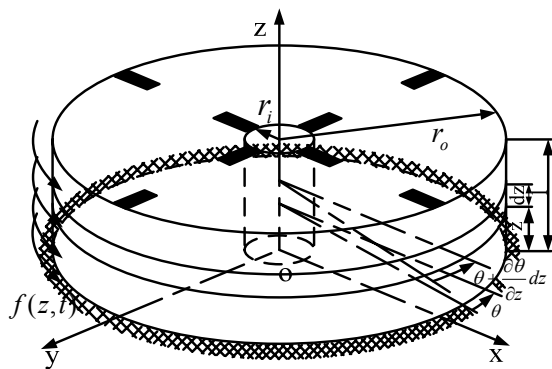


Fig. 4. Simplified mechanical model of upper E-type membrane.

It also simplifies lower E-type membrane into the model as shown in Fig. 5. The model is another straight circular shaft with constant section whose top is fixed and bottom is free under distributive torque $f(z,t)$. Due to the same size and stress, the coupling outputs are the same. So this paper analyzes torsional vibration problem of circular shaft in terms of the mechanical model as shown in Fig. 4.

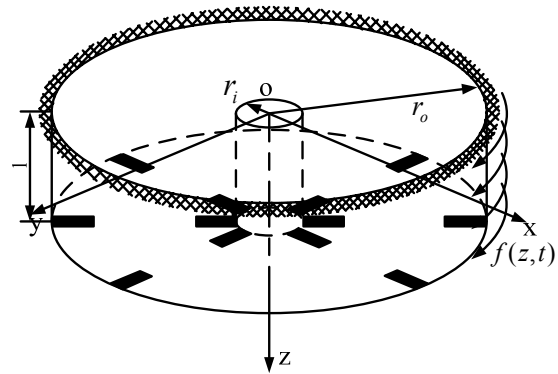


Fig. 5. Simplified mechanical model of lower E-type membrane.

3. Free Vibration Analysis of Torsion for Shaft

A micro section dz in the mechanical model as shown in Fig. 4 is taken and analyzed. $\theta(z,t)$ is the angular displacement in section z . The shaft twists under distributive torque $f(z,t)$. According to D'Alembert's principle, it is possible to obtain the partial differential equation (PDE) of torsional vibration for shaft:

$$I(z) \frac{\partial^2 \theta}{\partial t^2} - \frac{\partial}{\partial x} [GJ_\rho(z) \frac{\partial \theta}{\partial z}] = f(z,t) \quad (2)$$

where $I(z)$ is the moment of inertia per unit length. G is the shearing modulus of elasticity. $J_\rho(z)$ is the polar moment of inertia of the section. $I(z) = I = \text{constant}$, $J_\rho(z) = J_\rho = \text{constant}$, density $\rho(z) = \rho = \text{constant}$ and $I = \rho J_\rho$, if the density of the circular shaft is uniform. PDE (2) is reduced to:

$$\rho J_\rho \frac{\partial^2 \theta}{\partial t^2} - GJ_\rho \frac{\partial^2 \theta}{\partial z^2} = f(z,t) \quad (3)$$

Consider that the torsional vibration is free and $f(z,t) = 0$. Equation (2) can be expressed as the following form:

$$\frac{\partial^2 \theta}{\partial t^2} = a^2 \frac{\partial^2 \theta}{\partial z^2}, \quad (4)$$

where $a = \sqrt{G/\rho}$, it indicates the propagation velocity along z of shear elastic wave.

The characteristic of synchronous movement is able to be found by observing the free torsional vibration of shaft. It means that the general shape of the torsion angle for the shaft which is moving isn't changing when time is going, but the range of the general shape is changing when time is going. In the other words, each point which are moving reach the maximum range and pass the equilibrium position at the same time. In mathematical language, the angle function of describing torsion vibration $\theta(z, t)$ is separated in time and space. So the solution of boundary value problem can be expressed as followings:

$$\theta(z, t) = \Theta(z)F(t), \quad (5)$$

where $\Theta(z)$ indicates the modal shape function of torsional vibration for shaft. It is only connected with z . $F(t)$ indicates the vibration rule of the shaft. It is only connected with t . Insert Equation (5) into Equation (4), the equation becomes:

$$\frac{1}{F(t)} \frac{d^2 F(t)}{dt^2} = a^2 \frac{1}{\Theta(z)} \frac{d^2 \Theta(z)}{dz^2} \quad (6)$$

The foregoing equation relies on t on the left while it relies on z on the right. So it must be a constant equals to both sides while the foregoing equation is satisfied with any t and z . Assume this constant is $-\omega^2$, Equation (6) becomes the following two equations:

$$\frac{d^2 F(t)}{dt^2} + \omega^2 F(t) = 0 \quad (7)$$

$$\frac{d^2 \Theta(z)}{dz^2} + \beta^2 \Theta(z) = 0 \quad (8)$$

$$\beta = \frac{\omega}{a}, (0 < z < l)$$

It means that $F(t)$ must be simple harmonic, if synchronized motion is possible. So the solution of Equation (7) is:

$$F(t) = A \sin \omega t + B \cos \omega t = C \sin(\omega t + \varphi), \quad (9)$$

where A and B (or C and φ) are integration constant. They are decided by the initial conditions.

Assume the solution of Equation (8) is:

$$\Theta(z) = D \sin \beta z + E \cos \beta z, \quad (10)$$

where D and E are also the integration constants. They are decided by the boundary conditions.

By means of Equation (5), the solution of torsional free vibration while one section is fixed and the other one is free can be given by:

$$\theta(z, t) = (D \sin \beta z + E \cos \beta z) C \sin(\omega t + \varphi) \quad (11)$$

According to all kinds of analysis, the solution of torsional free vibration for shaft can be described by:

$$\theta(z, t) = \Theta(z) C \sin(\omega t + \varphi) \quad (12)$$

4. The Orthogonality of Mode Shape Functions

Equation (4) is rewritten into:

$$\rho J_\rho \frac{\partial^2 \theta}{\partial t^2} = G J_\rho \frac{\partial^2 \theta}{\partial x^2} \quad (13)$$

Taking the main vibration which Equation (12) indicates in Equation (13) results in the expression:

$$G J_\rho \Theta''(z) = -\omega^2 \rho J_\rho \Theta(z) \quad (14)$$

$\Theta_i(z)$ and $\Theta_j(z)$ can be assumed to be two different modal shape functions which are corresponding to the natural frequencies ω_i and ω_j . They have to satisfy Equation (14):

$$G J_\rho \Theta_i''(z) = -\omega_i^2 \rho J_\rho \Theta_i(z) \quad (15)$$

$$G J_\rho \Theta_j''(z) = -\omega_j^2 \rho J_\rho \Theta_j(z) \quad (16)$$

Both sides of Equation (15) are multiplied by $\Theta_j(z)$. Calculating the integration of z along axial length, it is possible to obtain:

$$\int_0^l G J_\rho \Theta_j(z) \Theta_i''(z) dz = -\omega_i^2 \int_0^l \rho J_\rho \Theta_j(z) \Theta_i(z) dz \quad (17)$$

In terms of integration by parts, the left side of Equation (17) can be written as:

$$\int_0^l G J_\rho \Theta_j(z) \Theta_i''(z) dz = G J_\rho [\Theta_j(z) \Theta_i'(z)]_0^l - \int_0^l \Theta_j'(z) \Theta_i'(z) dz \quad (18)$$

According to assumption of simple boundary condition, the endpoint is whether free or fixed. So $\Theta_j(z) = 0$ or $\Theta_i'(z) = 0$ ($z=0$ or l). Consequently, from Equation (17) and (18), we obtain:

$$\int_0^l GJ_\rho \Theta_j'(z) \Theta_i'(z) dz = \omega_i^2 \int_0^l \rho J_\rho \Theta_j(z) \Theta_i(z) dz \quad (19)$$

Due to the same way, we obtain:

$$\int_0^l GJ_\rho \Theta_j'(z) \Theta_i'(z) dz = \omega_j^2 \int_0^l \rho J_\rho \Theta_j(z) \Theta_i(z) dz \quad (20)$$

The modal shape function about the orthogonality of mass is deduced by Equation (19) subtracting Equation (20):

$$\int_0^l \rho J_\rho \Theta_i(z) \Theta_j(z) dz = 0 \quad i \neq j \quad (21)$$

The foregoing equation is a positive value when $i = j$. In terms of it, regularization of modal shape functions can be done. As $\Theta_i(z)$ and $\Theta_j(z)$ are taken as holomorphic modal shape functions, it can be expressed:

$$\int_0^l \rho J_\rho \Theta_i(z) \Theta_j(z) dz = \delta_{ij} \quad (22)$$

The modal shape function about the orthogonality of stiffness is deduced by Equation (17) and (21):

$$\int_0^l GJ_\rho \Theta_j(z) \Theta_i''(z) dz = 0 \quad (23)$$

The regularization of modal shape function is done by means of the foregoing equation, we obtain,

$$\int_0^l GJ_\rho \Theta_j(z) \Theta_i''(z) dz = -\omega_j^2 \delta_{ij} \quad (24)$$

where δ_{ij} is Kronig δ symbol. When $i = j$, δ_{ij} is 1. When $i \neq j$, δ_{ij} is 0.

5. Forced Vibration Analysis of Torsion for Shaft

Shaft is a continuous system of infinite degree of freedom (DOF). The solution of torsional forced vibration can depend on the superposition method of modal shapes, indicate the response of continuous system into series of modal shape functions and dispose the PDE of physical coordinates of the system as differential equations of motion (DEOM) of undamped single degree of freedom (SDOF) system. This paper imports the canonical coordinate $\eta_i(t)$. $\theta(z,t)$ which is the solution of Equation (3) with the given boundary conditions can be given by:

$$\theta(z,t) = \sum_{i=1}^{\infty} \Theta_i(z) \eta_i(t) \quad (25)$$

Since insert Equation (25) into PDE of torsional forced vibration for shaft (3), one has:

$$\sum_{i=1}^{\infty} \ddot{\eta}_i(t) \rho J_\rho \Theta_i(z) - \sum_{i=1}^{\infty} \eta_i(t) GJ_\rho \Theta_i''(z) = f(z,t) \quad (26)$$

Multiply both sides of Equation (26) by $\Theta_j(z)$ and calculate the integration of z along axial length, we obtain:

$$\sum_{i=1}^{\infty} \ddot{\eta}_i(t) \int_0^l \rho J_\rho \Theta_j(z) \Theta_i(z) dz - \sum_{i=1}^{\infty} \eta_i(t) \int_0^l GJ_\rho \Theta_j(z) \Theta_i''(z) dz = \int_0^l \Theta_j(z) f(z,t) dz \quad (27)$$

In terms of Equation (22) and (24), the foregoing equation is simplified into independent ordinary differential equations (ODE):

$$\ddot{\eta}_j(t) + \omega_j^2 \eta_j(t) = q_j(t) \quad (28)$$

which is called the j^{th} equation of canonical coordinate. Where $q_j(t) = \int_0^l \Theta_j(z) f(z,t) dz$ is the j^{th} generalized force of canonical coordinate. Due to Equation (28) is the same as the DEOM of undamped SDOF system under the external drive. So the response of it can be expressed as the following form:

$$\eta_j(t) = \frac{1}{\omega_j} \int_0^t q_j(\tau) \sin \omega_j(t-\tau) d\tau + \eta_j(0) \cos \omega_j t + \frac{\dot{\eta}_j(0)}{\omega_j} \sin \omega_j t \quad (29)$$

Taking the response of canonical coordinate as shown in Equation (29) in Equation (25) results in the response of shaft under the given initial condition and random excitation. If the initial conditions of torsional vibration for shaft is: $\eta_j(0) = 0$, $\dot{\eta}_j(0) = 0$ and the additional dynamic load is not the distributive torque $f(z,t)$, but the concentrated torque $M(t)$ which is located at ξ along axial length, the torsional forced vibration of shaft under zero initial condition can be expressed as:

$$\theta(z,t) = \sum_{j=1}^{\infty} \Theta_j(z) \eta_j(t) = \sum_{j=1}^{\infty} \frac{1}{\omega_j} \Theta_j(z) \Theta_j(\xi) \int_0^t M(\tau) \sin \omega_j(t-\tau) d\tau \quad (30)$$

6. Example

Because the simplified mechanical model of upper E-type membrane, with the help of the physical coordinate as shown in Fig. 3, the boundary condition can be given by:

$$\theta(0, t) = 0$$

$$\left. \frac{\partial \theta(x, t)}{\partial x} \right|_{x=l} = 0$$

Taking the foregoing boundary conditions in Equation (10) results in the expression of natural frequency and modal shape function of free vibration of upper E-type membrane:

$$\omega_i = \frac{(2i-1)\pi a}{2l} \quad i = 1, 2, \dots$$

$$\Theta_i(z) = D \sin \frac{(2i-1)\pi}{2l} z \quad i = 1, 2, \dots$$

In terms of the normalizing conditions of orthogonality in Equation (22) when $i = j$ and the modal shape functions of the foregoing equation, coefficient D is able to be calculated. The electromagnetic exciter is connected with 6-AFS which is studied in this paper by load cap that is seen as rigid body and apply loads on the elastomers in an indirect way, when it is under the condition of dynamic loads in M_z direction. A concentrated torque $M(t) = 2r_0 K \sin \omega t$ acts on the top edge of shaft. With the help of software MATLAB, the solution is shown as Table 2. (Considering the calculated amount and the accuracy of decoupling, this paper only chooses the first six order modal shapes.)

Table 2. Solution of free torsional vibration for the shaft.

j	ω_j	D	$\Theta_j(z)$	$\Theta_j(\xi)$
1	0.24477×10^7	191.42	$191.42 \sin(785.40z)$	191.42
2	0.73430×10^7	191.42	$191.42 \sin(2356.2z)$	-191.42
3	0.12238×10^8	191.42	$191.42 \sin(3927.0z)$	191.42
4	0.17134×10^8	191.42	$191.42 \sin(5497.8z)$	-191.42
5	0.22029×10^8	191.42	$191.42 \sin(7068.6z)$	191.42
6	0.26924×10^8	191.42	$191.42 \sin(8639.4z)$	-191.42

Due to the sensor is satisfied with zero initial condition based on the real working condition, the

response of forced torsional vibration for shaft can be obtain as follows:

$$\theta(z, t) = K(-1.0 \times 10^{-3} \sin 785.4z \frac{(2.0 \times 10^6 \sin \omega t - \sin(2.0 \times 10^6 t)\omega)}{(\omega - 2.0 \times 10^6)(\omega + 2.0 \times 10^6)} + 5.0 \times 10^{-4} \sin 2356.2z \frac{(7.0 \times 10^6 \sin \omega t - \sin(7.0 \times 10^6 t)\omega)}{(\omega - 7.0 \times 10^6)(\omega + 7.0 \times 10^6)}$$

$$- 0.3 \times 10^{-3} \sin 3927z \frac{(1.0 \times 10^7 \sin \omega t - \sin(1.0 \times 10^7 t)\omega)}{(\omega - 1.0 \times 10^7)(\omega + 1.0 \times 10^7)} + 2.0 \times 10^{-4} \sin 5497.8z \frac{(2.0 \times 10^7 \sin \omega t - \sin(2.0 \times 10^7 t)\omega)}{(\omega - 2.0 \times 10^7)(\omega + 2.0 \times 10^7)} - 2.0 \times 10^{-4} s$$

$$\sin 7068.6z \frac{(2.0 \times 10^7 \sin \omega t - \sin(2.0 \times 10^7 t)\omega)}{(\omega - 2.0 \times 10^7)(\omega + 2.0 \times 10^7)} + 1.0 \times 10^{-4} \sin 8639.4z \frac{(3.0 \times 10^7 \sin \omega t - \sin(3.0 \times 10^7 t)\omega)}{(\omega - 3.0 \times 10^7)(\omega + 3.0 \times 10^7)})$$

According to the basic assumption of elastic mechanics, only linear strain in radial direction ε_r , linear strain in circumferential direction ε_ϕ and angular strain $\gamma_{r\phi}$ are considered about circular thin plate. By analysis $\varepsilon_r = 0$ and $\varepsilon_\phi = 0$ under dynamic loads in M_z direction. According to the geometrical

relationship of deformation when the shaft twists, one has $\gamma_{r\phi} \approx \tan \gamma_{r\phi} = r \cdot d\theta / dz$.

In terms of the foregoing equation, the dynamic output when dynamic load in M_z direction acting on upper and lower E-type membranes is calculated as:

$$\gamma_{r\phi} = K(-1.2 \cos 785.4z \frac{(2.0 \times 10^6 \sin \omega t - \sin(2.0 \times 10^6 t)\omega)}{(\omega - 2.0 \times 10^6)(\omega + 2.0 \times 10^6)} + 1.2 \cos 2356.2z \frac{(7.3 \times 10^6 \sin \omega t - \sin(7.3 \times 10^6 t)\omega)}{(\omega - 7.3 \times 10^6)(\omega + 7.3 \times 10^6)}$$

$$- 1.2 \cos 3927z \frac{(1.2 \times 10^7 \sin \omega t - \sin(1.2 \times 10^7 t)\omega)}{(\omega - 1.2 \times 10^7)(\omega + 1.2 \times 10^7)} + 1.2 \cos 5497.8z \frac{(1.7 \times 10^7 \sin \omega t - \sin(1.7 \times 10^7 t)\omega)}{(\omega - 1.7 \times 10^7)(\omega + 1.7 \times 10^7)} - 1.2 \cos 7$$

$$068.6z \frac{(2.2 \times 10^7 \sin \omega t - \sin(2.2 \times 10^7 t)\omega)}{(\omega - 2.2 \times 10^7)(\omega + 2.2 \times 10^7)} + 1.2 \cos 8639.4z \frac{(2.7 \times 10^7 \sin \omega t - \sin(2.7 \times 10^7 t)\omega)}{(\omega - 2.7 \times 10^7)(\omega + 2.7 \times 10^7)})r$$

Due to Fig. 4 and 5, the resistance strain gauges are stuck on the circular thin plates. Assume that $z=l$ and the amplitude of dynamic loads K is 1,

figures of dynamic strain under different excitation frequencies are simulated with the help of software MATLAB (Fig. 6):

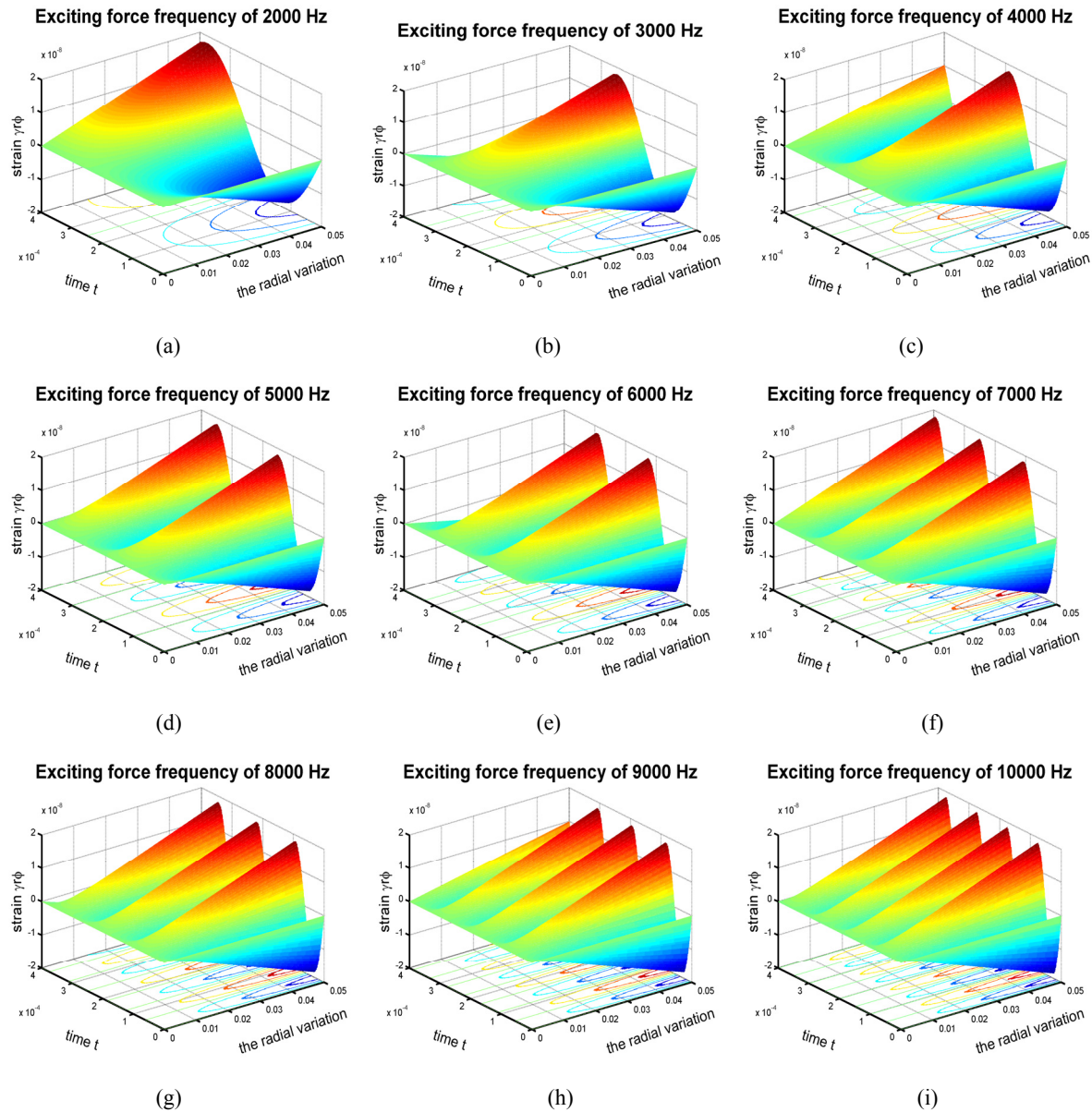


Fig. 6. Dynamic outputs of: (a) 5 Hz, (b) 10 Hz, (c) 15 Hz, (d) 20 Hz, (e) 25 Hz, (f) 30 Hz, (g) 100 Hz, (h) 200 Hz, (i) 300 Hz. (xlabel: the radial variation, ylabel: time t , zlabel: strain $\gamma_{r\phi}$)

7. Conclusions

This paper takes six-axis force sensor based on double layer E-type membrane for example. Upper and lower E-type membranes are simplified into a straight circular shaft with constant section. The dynamic strain is calculated and the figures of dynamic strain are plotted on the basis of the fundamental theory of mechanical vibration, vibration mechanics and elastic mechanics.

The dynamic output provides data for data processing. Dynamic characteristics can also be extracted from the data. The course of solving this

problem provides a theoretical foundation for dynamic decoupling of six-axis force sensor and dynamic compensation. It also has a significance to improve the dynamic response speed of the sensor.

Acknowledgment

The authors would like to thank the financial supports from National Natural Science Foundation of China (Grant No. 51175001) and Anhui Provincial Natural Science Foundation (Grant No. 11040606M144).

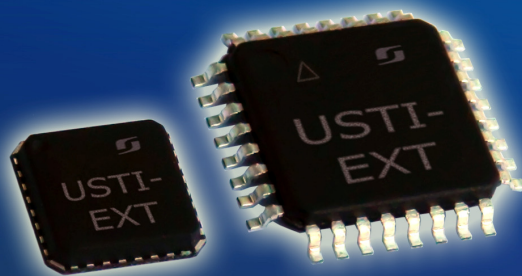
References

- [1]. Z. S. Liu, Y. Wang, E. W. Chen, W. Li, Y. J. Ge, A method for measuring dynamic performance index of robot's multi-axis wrist force sensor, in *Proceedings of the IEEE International Conference on Information Acquisition*, 2005, pp. 170-174.
- [2]. D. Z. Xu, Z. C. Wu, Y. J. Ge, F. Shen, Y. Ge, The solution to and the analysis with cross-coupling matrix of six-axis wrist force sensor for robot, *Chinese Journal of Scientific Instrument*, Vol. 26, Issue 1, 2005, pp. 75-81.
- [3]. Q. K. Liang, D. Zhang, Q. J. Song, Y. J. Ge, H. B. Cao, Y. Ge, Design and fabrication of a six-dimensional wrist force/torque sensor based on E-type membranes compared to cross beams, *Measurement*, Vol. 43, 2010, pp. 1702-1719.
- [4]. K. J. Xu, C. Li, Dynamic decoupling and compensating methods of multi-axis force sensors, *IEEE Transactions on Instrumentation and Measurement*, Vol. 49, Issue 5, 2000, pp. 935-941.
- [5]. A. G. Song, J. Wu, J. Q. Li, Q. J. Zeng, W. Y. Huang, A novel four degree-of-freedom wrist force/torque sensor with low coupled interference, in *Proceedings of the IEEE/RSJ International Conference on Intelligent Robots and Systems*, 2006, pp. 4423-4428.
- [6]. P. A. A. Laura, E. Romanelli, Fundamental frequency of transverse vibration of a circular annular plate of rectangular orthotropy with an intermediate circular support, *Journal of Sound and Vibration*, Vol. 215, Issue 2, 1998, pp. 390-394.
- [7]. Z. H. Zhou, K. W. Wong, X. S. Xu, A. Y. T. Leung, Natural vibration of circular and annular thin plates by Hamiltonian approach, *Journal of Sound and Vibration*, Vol. 330, 2011, pp. 1005-1017.
- [8]. S. Stoykov, P. Ribeiro, Periodic geometrically nonlinear free vibrations of circular plates, *Journal of Sound and Vibration*, Vol. 315, 2008, pp. 536-555.
- [9]. Vinayak Ranjan, M. K. Ghosh, Transverse vibration of thin solid and annular circular plate with attached discrete masses, *Journal of Sound and Vibration*, Vol. 292, 2006, pp. 999-1003.
- [10]. X. H. Deng, W. C. Yang, H. H. Shen, Y. Yu, Y. J. Ge, J. Su, A distributing and decoupling method of microminiature multi-dimension robot finger force sensor, in *Proceedings of the IEEE International Conference on Robotics and Biomimetics*, 2007, pp. 15-18.

2013 Copyright ©, International Frequency Sensor Association (IFSA). All rights reserved.
(<http://www.sensorsportal.com>)

Universal Sensors and Transducers Interface (USTI-EXT) for extended temperature range

-55 °C ... +150 °C



26 measuring modes for all frequency-time parameters,
rotational speed, capacitance Cx, resistance Rx, resistive bridges
Frequency range, 0.05 Hz ... 7.5 MHz (120 MHz);
Programmable relative error, % 1 ... 0.0005 %
Conversion speeds 6.25 us ... 12.5 ms
SPI, I2C, RS232 (master and slave, up to 76 800 baud rate)
Packages: 32-lead, 7x7 mm TQFP and 32-pad, 5x5 mm (QFN/MLF)

Applications: automotive industry, avionics, military, etc.

<http://www.techassist2010.com/> info@techassist2010.com